

A novel approach to medical radioisotope production using inverse kinematics: A successful production test of the theranostic radionuclide ^{67}Cu



G.A. Souliotis^{a,*}, M.R.D. Rodrigues^{b,e}, K. Wang^b, V.E. Iacob^b, N. Nica^b, B. Roeder^b, G. Tabacaru^b, M. Yu^c, P. Zanotti-Fregonara^c, A. Bonasera^{b,d}

^a Laboratory of Physical Chemistry, Department of Chemistry, National and Kapodistrian University of Athens, Athens, 15771, Greece

^b Cyclotron Institute, Texas A&M University, College Station, TX, 77843, USA

^c Houston Methodist Research Institute, Houston, TX, 77030, USA

^d Laboratori Nazionali del Sud, INFN, Catania, 95123, Italy

^e Instituto de Física, Universidade de São Paulo, São Paulo, 05508-090, Brazil

HIGHLIGHTS

- Production of the theranostic radionuclide ^{67}Cu in inverse kinematics.
- Production reaction: ^{70}Zn (15 MeV/nucleon) beam on a hydrogen gas target.
- Obtained activity of ^{67}Cu and other coproduced radioisotopes. Compared with theoretical estimates.
- Discussion of optimization steps to produce ^{67}Cu and other medical radioisotopes in inverse kinematics.

ABSTRACT

A novel method for the production of important medical radioisotopes has been developed. The approach is based on performing the nuclear reaction in inverse kinematics, namely sending a heavy-ion beam of appropriate energy on a light target (e.g. H, d, He) and collecting the isotope of interest. In this work, as a proof-of-concept, we studied the production of the theranostic radionuclide ^{67}Cu ($T_{1/2} = 62$ h) via the reaction of a ^{70}Zn beam at 15 MeV/nucleon with a hydrogen gas target. The ^{67}Cu radionuclide alongside other coproduced isotopes, was collected after the gas target on an aluminum catcher foil and their radioactivity was measured by off-line γ -ray analysis. After 36 h post irradiation, apart from the product of interest ^{67}Cu , the main radioimpurity coming from the $^{70}\text{Zn} + p$ reaction was ^{69m}Zn ($T_{1/2} = 13.8$ h), which can be reduced by further radio-cooling. Moreover, along with the radionuclide of interest produced in inverse kinematics, the production of additional radioisotopes is possible by making use of the forward-focused neutrons from the reaction and allowing them to interact with a secondary target. A preliminary successful test of this concept was realized in the present study. The main requirement to obtain activities appropriate for preclinical studies is the development of high-intensity heavy-ion primary beams.

1. Introduction

Medical radionuclides play a central role in nuclear medicine in the fields of diagnostic imaging and radioimmunotherapy (RIT) (Qaim (2017); Srivastava (2014); Stocklin et al. (1995)). Radionuclides emitting low-range highly ionizing radiation (β^- or α particles, Auger or conversion electrons) are essential for RIT approaches. Apart from several standard radionuclides, currently the β^- emitters ^{47}Sc ($T_{1/2} = 3.4$ d), ^{67}Cu ($T_{1/2} = 2.6$ d), ^{105}Rh ($T_{1/2} = 1.5$ d), ^{161}Tb ($T_{1/2} = 6.9$ d) and ^{186}Re ($T_{1/2} = 3.7$ d) (Champion et al. (2016); Qaim (2017)) are becoming increasingly interesting.

Specifically, ^{67}Cu , the longest-lived radioisotope of copper, is ideally suited for both radioimmunotherapy and imaging for several

reasons (Asabella et al. (2014)). First, from a chemical perspective, copper is an essential trace element for most organisms and specifically for humans as it takes part in important biochemical processes (Linder (1991)). The coordination chemistry of Cu has been well established (Price and Orvig (2014)). Copper can be linked to antibodies, proteins and other biologically important molecules (Follacchio et al. (2018); Ting et al. (2009); Schubiger et al. (1996); Sugo et al. (2017)). The nuclide ^{67}Cu can be combined with the same type of radiopharmaceuticals as ^{64}Cu ($T_{1/2} = 12.7$ h) or ^{61}Cu ($T_{1/2} = 3.3$ h), leading to efficient theranostic pairs (Zimmermann et al. (2003)).

The half-life of ^{67}Cu (62 h) is appropriate to deliver a high dose rate to the tumor. Furthermore, its β^- decay ($E_{\text{e},\text{max}} = 577$ keV) is followed by the emission of soft γ radiation of 185 keV (48.7%), 93 keV (16%)

* Corresponding author.

E-mail address: soulioti@chem.uoa.gr (G.A. Souliotis).

and 91 keV (7%). This makes ^{67}Cu suitable for imaging the radiotracer distribution by single-photon emission computed tomography (SPECT) using the cameras widely developed for the 140 keV γ rays of ^{99m}Tc . Compared to the standard RIT radioisotope ^{90}Y ($T_{1/2} = 64$ h, $E_{e,max} = 2280$ keV), which is a pure β^- emitter, ^{67}Cu offers the possibility of SPECT imaging and treatment of smaller size tumors (up to 4 mm, compared to 12 mm in the case of ^{90}Y). In addition, ^{67}Cu compares favorably with another standard radioisotope, ^{131}I ($T_{1/2} = 8.0$ d, $E_{e,max} = 610$ keV), which has a longer half-life and emits higher energy γ rays (364 keV, 82%) and thus, may increase the undesired dose to the patient and the medical personnel.

It is noteworthy that while the other radioisotopes of copper, especially ^{64}Cu , have already been used in radiopharmaceuticals for a wide range of preclinical and clinical studies (Follacchio et al. (2018); Peng et al. (2006)), ^{67}Cu has been used in a rather limited number of studies, albeit with very promising results (Jin et al. (2017); Katz and Barnea (1990); Knogler et al. (2007); Novak-Hofer and Schubiger (2002)). The main factor limiting wider preclinical and clinical use is its limited availability (Smith et al. (2012)).

The production of ^{67}Cu in nuclear reactors started about 50 years ago (O'Brien (1969)) and continues until the present at several reactor facilities (e.g. Johnsen et al. (2015); Uddin et al. (2014); Mirzadeh et al. (1986)). Recently, however, the main focus has shifted to methods based on particle accelerators (Smith et al. (2012)). Presently, the main production route is via the reaction $^{68}\text{Zn}(p, 2p)^{67}\text{Cu}$ (Katabuchi et al. (2008); Medvedev et al. (2008); Pupillo et al. (2018); Stoll et al. (2002)). This approach is based on the use of intense medium-energy ($E_p = 70\text{--}100$ MeV) proton beams that are produced by several particle accelerators, including medium-energy cyclotrons. However, these multipurpose facilities cannot dedicate all their beam time to radioisotope production.

Other production routes based on lower-energy charged particle reactions are $^{70}\text{Zn}(\alpha, p)^{67}\text{Cu}$ (Hilgers et al. (2003); Jamriska et al. (1995); Kastleiner et al. (1999)), $^{70}\text{Zn}(d, \alpha n)^{67}\text{Cu}$ (Kozempel et al. (2012)) and $^{nat}\text{Zn}(d, x)^{67}\text{Cu}$ (Hosseini et al. (2017)), $^{64}\text{Ni}(\alpha, p)^{67}\text{Cu}$ (Ohya et al. (2018); Skakun and Qaim (2004)). Moreover, production routes based on reactions induced by accelerator-produced neutrons have been applied (Kawabata et al. (2015); Kin et al. (2013); Sato et al. (2014); Spahn et al. (2004)). In addition, ^{67}Cu has been produced in photonuclear reactions using bremsstrahlung photons from high-intensity electron linacs (Gopalakrishna et al. (2018); Starovoitova et al. (2014, 2015); Yagi and Kondo (1978)).

In addition to the aforementioned traditional approaches, isotope harvesting in projectile fragmentation facilities has been suggested as an alternative source of medical isotopes. A proof-of-concept was presented in the recent work by Mastren et al. (Mastren et al. (2014, 2015)) at the National Superconducting Cyclotron Laboratory (NSCL). This work involved harvesting and separation of ^{67}Cu from a mixture of projectile fragments stopped in an aqueous beam-collection system. The ^{67}Cu radionuclide separation was followed by radiolabelling and bio-distribution studies.

A general characteristic of all the traditional production methods is the fact that the desired radioisotope of ^{67}Cu is produced inside the target material which can be moderately or highly expensive, depending on the setup and approach. In regard to the production of ^{67}Cu , the natural abundances of ^{68}Zn , ^{70}Zn , and ^{64}Ni are 18.45%, 0.61%, and 0.93%, respectively. Thus, in these cases, an efficient analysis scheme is necessary for the collection of the desired ^{67}Cu isotope and recovery of the target material for subsequent reuse in the production scheme (Smith et al. (2012)). Along with this traditional scheme, in the isotope-harvesting route, the isotope of interest has to be separated from a very broad range of radioisotopes of other elements that are abundantly coproduced in a projectile fragmentation reaction. Thus, an appropriate multistep separation process is necessary (Mastren et al. (2015)).

In this paper, we present an innovative approach for the production of medical radioisotopes based on inverse-kinematics nuclear reactions,

namely, sending a heavy-ion beam on a light target and collecting the radioisotope after the target. The main advantage of using an inverse kinematics reaction is that the products are strongly focused along the beam direction and, thus, can be relatively easily collected for immediate use. It is our intention to explore the possible complementarity of our method to the traditional production paths and pave the way to further developments.

Proof-of-principle of the aforementioned approach is presented for the production of ^{67}Cu via the reaction of a ^{70}Zn beam at 15 MeV/nucleon with a hydrogen gas target. This work demonstrates that important non-standard medical radioisotopes with high radionuclide purity can be produced, provided that low-energy and high-intensity primary beams are available. Our method has some similarity with the isotope-harvesting approach from fragmentation facilities, in the sense that, in the latter, the fragmentation reactions also occur in inverse kinematics, albeit at high energies (above 100 MeV/nucleon), producing a very broad range of isotopes. Our inverse kinematics approach, however, takes place at low energy. From a reaction point of view, inverse kinematics, of course, corresponds to an inversion of the reference frame, compared to the traditional approach of direct kinematics, i.e., light projectile on heavy target. Consequently, the cross sections of a given channel are the same in the two approaches at the same energy in the center of mass. Furthermore, by choosing the energy range to favor a desired reaction channel, the radionuclide of interest can be selectively produced with minimal radioimpurities and implanted in an appropriate catcher material for subsequent use (after minimal radiochemical processing, if necessary). Concomitantly, the forward-focused neutrons from the primary reaction can be sent to a secondary target for additional radioisotope production.

The structure of the paper is as follows: in section 2, we present the experimental setup and the measurements; in section 3, we continue with the data analysis and the results. In section 4, we discuss improvements of the present method and further plans. Finally, in section 5, we provide a summary and conclusions.

2. Experimental setup and measurements

The experimental work took place at the Cyclotron Institute of Texas A&M University (TAMU). A primary beam of $^{70}\text{Zn}^{15+}$ from the ECR source was accelerated by the K500 superconducting cyclotron to an energy of 15 MeV/nucleon and transported to the target chamber of the MARS recoil separator (Tribble et al. (1989)). The beam impinged on a cryogenic gas cell filled with H_2 gas held at a pressure of 2.7 atm in contact with a liquid nitrogen reservoir (Brinkley et al. (2009)). The cryogenic gas cell (Fig. 1) had a length of 10 cm with $4\text{ }\mu\text{m}$ Havar entrance and exit windows of 19.0 mm diameter. A magnetic stirring system (referred to as “magnetic exciter” in Fig. 1) was operated to provide circulation of the gas. The experimental setup is schematically shown in Fig. 2. An aluminum catcher foil, placed after the hydrogen gas cell, was used to collect the produced ^{67}Cu nuclei, along with other coproduced nuclides, from the reaction of the ^{70}Zn beam with the proton target. The Al catcher foil was mounted on a rectangular aluminum target frame with a 12.7 mm diameter hole. We note that with this setup, the catcher foil can be removed from the frame after the irradiation period and be counted (as described in 3.1). Also, the frame itself can be separately counted to infer possible angular spread of ions of interest (see section 3.2).

The irradiation lasted 6.5 h with a beam current of 0.31 pA (particle nA) (2.0×10^9 particles s^{-1}). The current was periodically monitored and was nearly constant (within 15%). The measurement of the current was performed by inserting a Faraday cup mounted on the same target ladder as the Al catcher frame. The measurement of the beam current at this location (i.e. after the gas cell) was 8.0 nA of ^{70}Zn (7.0 MeV/nucleon) at an average charge state of 26+. (We note that ions traversing material at a given velocity are characterized by an equilibrium charge state distribution given by various empirical or semi-

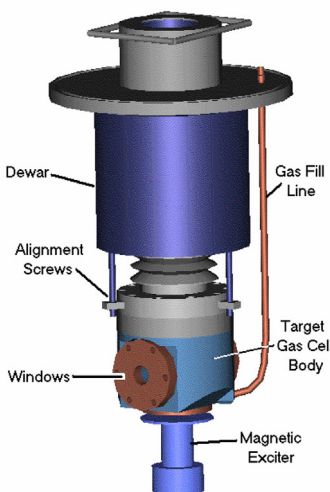


Fig. 1. (Color online) The cryogenic gas target cell used in the present work (Brinkley et al. (2009)). (For interpretation of the references to colour in this figure legend, the reader is referred to the Web version of this article.)

empirical systematics.) The equilibrium charge state of ^{70}Zn ions at 7.0 MeV/nucleon was calculated with the parametrization of Leon et al. (Leon et al. (1998)). After 36.4 h from the end of the irradiation, the Al catcher foil was placed in front of a high-purity germanium (HPGe) detector for off-line γ -ray analysis as described in the following sections.

3. Data analysis and results

3.1. Off-line γ -ray analysis

The radioactivity of the produced ^{67}Cu and the other coproduced radioisotopes was determined by off-line analysis of the γ -ray spectra. The foil was placed at a distance of $d = 17.2(10)$ mm from the end cap of the detector. Under this condition, the dead time of the counting system was around 2–3%, thus avoiding the pile-up effect. The energy resolution of the detector system was 2.5–4.0 keV (FWHM) for the peaks of interest.

The energy calibration was performed using known γ -rays obtained in the spectra. The absolute photopeak efficiencies for the actual source-detector geometry were obtained with the Monte Carlo codes GEANT4 (Agostinelli et al. (2003)) and EGSnrc (Kawrakow et al. (2000), Kawrakow and Rogers (2003)). The spectrum of the room background was measured for 67.3 h.

The radioactivity levels of the isotopes were determined by the

quantification of the photopeaks of the γ -rays taking into account the branching ratios and the absolute efficiencies of the detector. A detailed description of the γ -ray analysis of all the observed γ -ray peaks will be presented in Rodrigues et al. (2019).

In Fig. 3, we present the background-subtracted γ -ray spectrum obtained during an accumulation period of 68.0 h, starting 36.4 h after the end of the irradiation. We note that the peaks at 92 keV and 185 keV are characteristic of ^{67}Cu decay. The peak at 439 keV is due to the main radioimpurity of ^{69m}Zn ($T_{1/2} = 13.8$ h) from the $^{70}\text{Zn} + p$ reaction. We observe a small contribution, around 3% of the ^{67}Cu production, from the γ -ray at 300.2 keV characteristic of the presence and decay of ^{67}Ga ($T_{1/2} = 78$ h) with a branching ratio of 16.7%. We note that this radioimpurity, decaying to the same levels of ^{67}Zn as ^{67}Cu , is intensely coproduced in the main production route via $^{68}\text{Zn}(p, 2p)^{67}\text{Cu}$ with high energy protons (Smith et al. (2012)). This γ -ray for ^{67}Cu has a branching ratio of only 0.8%. Similarly, the peak at 1115.5 keV, characteristic of ^{65}Zn ($T_{1/2} = 244$ d), is significantly suppressed (0.2% of the ^{67}Cu production). This radionuclide is notoriously produced in the high-energy ^{67}Cu production methods and requires radiochemical separation.

In the spectrum depicted in Fig. 3, we observe peaks from a series of radionuclides that are mainly due to nuclear reactions on the Havar windows and the Al catcher foil. More specifically, the radionuclides ^{86}Y , ^{87}Y , ^{89}Zr , ^{90}Nb and ^{93m}Mo are fusion-evaporation products of the reaction $^{70}\text{Zn} + ^{27}\text{Al}$ (with the beam of ^{70}Zn entering the Al catcher at 7.0 MeV/nucleon, see section 3.2). Furthermore, the heavier radionuclides ^{111}In , ^{117m}Sn and ^{119}Te are residues of the reaction of the ^{70}Zn beam with the constituents of the Havar alloy (42% Co) of the gas-cell windows. We also identified the presence of ^{7}Be ($T_{1/2} = 53$ d, $E_{\gamma} = 477.6$ keV) possibly coming from the activation of the small Be or C content of the Havar alloy (0.02–0.08% and 1.6%, respectively). A complete analysis of the origin and the activity of these radionuclides will be presented in (Rodrigues et al. (2019)). As we discuss in section 3.2, the radioimpurities coming from the Havar windows and the Al catcher foil can be reduced or eliminated by proper tuning of the energy loss of the primary beam in the gas cell, so they may not present a potential problem in the proposed method of radionuclide production.

From this analysis, the activity of the produced ^{67}Cu at the end of the 6.5 h of irradiation was 1.6(5) kBq with the beam current of 0.31 pA. This leads to a specific activity of 0.8(3) kBq/h/pnA (or equivalently, 0.8(3) MBq/h/p μ A).

Along with the activity of ^{67}Cu , we report the measured activity of 0.094 kBq of the ^{69m}Zn ($T_{1/2} = 13.8$ h) at the end of the irradiation (this corresponds to a specific activity of 0.045 kBq/h/pnA). This is a rather low activity that can be further reduced by an appropriate cooling period (of 2 days, for example). In brief, at this initial development stage of our approach and following common practice, we may consider the level of the radioimpurities (^{69m}Zn , ^{67}Ga , and ^{65}Zn) coming from the

Irradiation setup for ^{67}Cu production in inverse kinematics

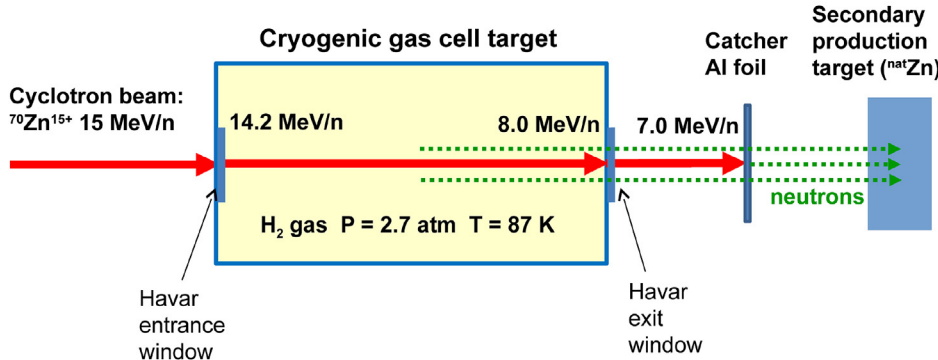


Fig. 2. (Color online) Schematic diagram of the irradiation setup. A ^{70}Zn beam at 15 MeV/nucleon enters the gas cell and interacts with the hydrogen gas. The heavy reaction products, including ^{67}Cu , after exiting the gas cell are implanted in the Al catcher. The energies of the beam are listed as it passes through the entrance window, the gas and the exit window (thick red arrows). The dashed (green) arrows represent the neutrons produced via the interactions of the ^{70}Zn beam with the hydrogen gas and the Al catcher. For details, see sections 2, 3.2, and 3.3. (For interpretation of the references to colour in this figure legend, the reader is referred to the Web version of this article.)

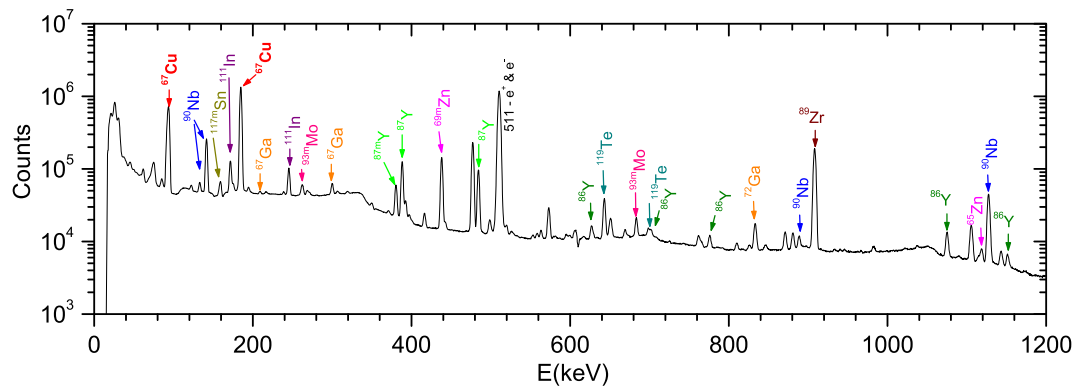


Fig. 3. (Color online) Typical background-subtracted gamma-ray spectrum of the Al catcher foil following the interaction of a ^{70}Zn (15 MeV/nucleon) beam with the hydrogen gas cell after 36.4 h from the end of the irradiation. The peaks are labelled with the corresponding radionuclides (see text). We specifically note the two peaks (at 92 keV and 185 keV) due to ^{67}Cu and the peak (at 439 keV) due to ^{69m}Zn ($T_{1/2} = 13.8$ h), which is the main radioimpurity coming from the production reaction $^{70}\text{Zn} + \text{p}$. (For interpretation of the references to colour in this figure legend, the reader is referred to the Web version of this article.)

main reaction $^{70}\text{Zn} + \text{p}$ as acceptable (see also relevant discussion in section 4).

3.2. Comparison of measured ^{67}Cu activity with estimates

In this section, we estimate the activity of the radionuclide ^{67}Cu produced in the inverse kinematics reaction ^{70}Zn (15 MeV/nucleon) + p. The cross sections for the direct kinematics reaction ^{70}Zn (p, α) ^{67}Cu have been reported in Kastleiner et al. (1999). We take into account that the 10 cm long gas target cell was filled with H_2 gas at a pressure of 2.7 atm and a temperature of about 87 K via the thermal contact with the LN_2 Dewar. Under these conditions, the H_2 gas target thickness was 7.5 mg/cm². Using the code SRIM (Ziegler et al. (2013)), we calculated the energy losses of the beam in the entrance window, the gas and the exit window of the gas cell. The ^{70}Zn beam hit the entrance window at 15 MeV/nucleon, exited it at 14.2 MeV/nucleon, traversed the gas and reached the exit window at 8.0 MeV/nucleon and, finally exited it at 7.0 MeV/nucleon (Fig. 2). For convenience, we reported the energies of the beam in MeV/nucleon, as customary for heavy-ion beam physics. From these, of course, total energies and energy losses can be easily inferred. Furthermore, we note that at the present energies, the lateral straggling of the beam and the heavy reaction products is very small, that we practically consider it negligible.

Using the data of Kastleiner et al. (Kastleiner et al. (1999)), we estimated the integral of the excitation function in the region 14.2–8.0 MeV, resulting in an average value for the cross section of 7.5 mb for ^{67}Cu . Using this cross section value and the H_2 gas target thickness, we obtained the production rate of ^{67}Cu . Subsequently, we obtained the produced activity, assuming 1 h of irradiation with a beam intensity of 1 pnA. This activity is calculated to be 1.8 kBq/h/pnA (or equivalently, 1.8 MBq/h/ μA). We notice that the measured activity of 0.8(3) kBq/h/pnA is about 2.2 times lower than the expected activity, as obtained with the previously described procedure.

In this section, we discuss several possible sources giving rise to the discrepancy between the experimental and the theoretical activity of ^{67}Cu : a) the spread of the recoiling ^{67}Cu nuclei that may result in an incomplete collection on the Al catcher foil. As previously noted, the Al catcher foil was mounted on an Al frame with a 12.7 mm hole. The ^{67}Cu activity of the target frame was measured to be 0.12 kBq which is 7.5% of the main activity collected on the Al catcher foil; b) the use of an unsuppressed Faraday cup to measure the beam current. As it is well known, the sputtering of electrons from the side of the Faraday cup hit by the heavy-ion beam results in an increase of the measured positive current leading to a decrease of the obtained production rate and, thus, the specific activity. The cup should be biased to a positive voltage (in the range 200–400 V). Such electron suppression of the Faraday cup

was not performed in the present experiment. This effect may account for about 20–30% of the discrepancy, but it should be quantified for the present heavy-ion setup (as performed in Carzaniga et al. (2017), Fig. 4, for proton beams); c) the reduction of the pressure of the H_2 gas due to local heating along the path of the primary beam. As reported in a previous study (Brinkley et al. (2009)), this effect has been observed in the behavior of this gas cell during its use for radioactive beam production with the MARS recoil separator. The rate of radioactive beams has been observed to drop when intense primary beams were used, but no quantitative estimates were reported there. We mention that in the recent works of Iacob et al. (2006, 2010), operation of the gas cell under periodic beam irradiation (beam-on – beam-off cycles lasting seconds) showed a transient drop of the beam intensity at the beginning of each cycle. A related quantitative account of this effect under continuous beam irradiation was reported by Amadio et al. (Amadio et al. (2008)) for the production of a low-energy radioactive beam of ^7Be in a cryogenic hydrogen gas cell. In that setup, circulation of the hydrogen gas cooled at LN_2 temperature indicated that the effect of the local pressure reduction may amount to 60–70% at high primary beam currents [Fig. 4 of (Amadio et al. (2008))]. Similar measurements are necessary for the present gas cell under continuous irradiation with the relevant heavy-ion beams.

Finally, we mention that, by using the cross section data of (Kastleiner et al. (1999)), the production cross section of ^{67}Cu drops to nearly zero at about 7 MeV. Thus, in the energy range 14.2–8.0 MeV/nucleon of the ^{70}Zn beam in the hydrogen gas, almost the full thickness of the target was exploited to produce ^{67}Cu .

3.3. Use of the neutrons from the primary reaction for secondary radioisotope production

The interaction of ^{70}Zn at 15 MeV/nucleon with the proton target produces about 1.6 neutrons per reaction, as calculated with the code TALYS (Koning and Rochman (2012); Duchemin et al. (2015)). Along with the heavy reaction products, these neutrons are also kinematically focused in the forward direction and can be exploited for further radioisotope production by simply letting them interact with a secondary target, e.g., a ^{68}Zn or ^{nat}Zn target for additional production of ^{67}Cu . In this study, we performed such a test by placing a block of twenty $25.4 \times 25.4 \text{ mm}^2$ foils of ^{nat}Zn with 1 mm thickness behind the Al catcher (Fig. 2).

Because this production arises from the secondary neutrons, the specific activity is expected to be about 2 orders of magnitude lower than the main production channel. However, given the long mean free path of the neutrons (with a typical value of several cm), production of different isotopes is conceivable with these neutrons impinging on

different targets. This production scheme shares some similarity with the one recently published in (Auditore et al. (2017)) employing secondary neutrons from the target of a standard ^{18}F radioisotope-producing setup. The advantage of our inverse kinematics approach is the strong focusing of the secondary neutrons, which can be directed to a target stack of much smaller size than the one used in (Auditore et al. (2017)), which essentially encloses the target. The results of our neutron-production test are promising. The analysis work is currently in progress and will be presented in Rodrigues et al. (2019). For completeness, we mention that, along with the neutrons, 0.13 protons and 0.02 alpha particles are produced per reaction according to TALYS. However, the protons and the alphas may be considered insignificant for secondary isotope production due to their low yield and their short mean free path (range) compared to the neutrons.

4. Discussion and future plans

The present preliminary study that we performed at the Cyclotron Institute of TAMU confirms that important medical radionuclides, such as ^{67}Cu , can be effectively produced using inverse kinematics. The main advantages of the present novel approach along with necessary developments and relevant implementations are discussed below.

First, the produced radionuclides are strongly focused along the beam direction and, thus, can be easily collected. In this respect, it is possible to minimize the production of radioimpurities arising from the main reaction by choosing the appropriate reaction channel(s) and the subsequent cooling time of the products. Moreover, it is possible to minimize the radioimpurities resulting from the primary beam interacting with the Havar windows of the gas target and the catcher material. Of course, we cannot avoid reactions at the entrance window, where the beam enters with the full energy of 15 MeV/nucleon and induces reactions on the foil. However, the products coming from peripheral or semiperipheral (deep-inelastic) collisions on the isotopes of Havar (Co, Cr, Ni, W, etc.) have rather wide angular distributions [e.g., (Fountas et al. (2014)) and (Papageorgiou et al (2018)) Fig. 4] and are expected to mostly miss the catcher foil (depending on its diameter). On the other hand, the products of complete or nearly complete fusion are forward-focused, but are heavier and slower than the beam and, thus, may mostly stop in the gas.

Regarding the exit window, it is possible to adjust the gas cell parameters (pressure, temperature and length) so that the primary beam reaches this window at low energy, i.e. near or below the Coulomb barrier of the relevant reactions (e.g., 4.0 MeV/nucleon). Consequently, nuclear reactions can be suppressed or fully eliminated on that window. Of course, under these conditions, the low energy primary beam exiting the gas cell will not induce reactions in the catcher material. For example, regarding the $^{70}\text{Zn} + ^{27}\text{Al}$ reaction, the Coulomb barrier corresponds to a projectile energy of 3.5 MeV/nucleon. We understand that detailed simulations and further experimental tests are necessary to achieve optimum conditions for the experimental setup and production procedure. Under properly fine-tuned conditions, water or other materials (salt, sugar, etc.) can be used to collect the radioisotopes in a convenient chemical form, so that, post radiolabelling, they may be used for tests on animals.

According to our estimates, with a primary beam of 1 particle μA , we can reach activities of 1.8 MBq/h and, thus, obtain milliCurie quantities of ^{67}Cu within 24 h of irradiation. The μA heavy-ion beam intensities are achievable with contemporary ion-source and accelerator technology. Under such intense heavy-ion beam irradiation, apart from the radioimpurities already mentioned, we should consider the quantities of stable isotopes implanted in the catcher material. Most importantly, the unreacted ^{70}Zn beam, with intensity 1 particle μA , corresponds to implantation of about 1 $\mu\text{mol}/\text{day}$. Specifically for the case of Zn, this quantity may be considered biochemically insignificant to an initial class of applications. Regarding the stable reaction products (which, of course, cannot be quantified with γ -decay spectroscopy), we

may rely on the TALYS calculation for a first estimate. For the $^{70}\text{Zn} + \text{p}$ reaction in the energy range of 14–7 MeV/nucleon, we found that the most important stable isotope is ^{69}Ga produced with average cross section of 400 mb, corresponding to 2 nmol/day of Ga implantation in the catcher. Again, to a first approximation, this may be considered as biochemically insignificant. However, at a later development stage, we may consider a standard radiochemical process to separate ^{67}Cu from Zn and Ga isotopes (either radioactive or stable) that are co-implanted in the catcher material (Smith et al. (2012)).

As we briefly mentioned, secondary neutrons from the primary reaction can be used to irradiate other targets for further radioisotope production of the same or different type (e.g. Cu, Sc, etc.). However, in this case, radiochemical methods are needed to separate the medical radionuclides, as in the traditional production schemes (Smith et al. (2012)).

From a financial point of view, material costs may be considerably reduced, since the heavy (and usually rare) element is used as the projectile (for instance, ^{70}Zn has 0.6% natural abundance). We note that the typical quantity of solid material used in the oven of an ECR ion source is of the order of mg/day for the development and delivery of intense heavy-ion beams. This quantity is to be compared to the gram quantities for the target material in the standard approach (which, of course, must be recycled in the case of expensive separated isotopes). Also, the radiochemical processing may be substantially minimized or, desirably, eliminated because the radioisotope of interest is collected and essentially used directly after production (and appropriate cooling). However, the primary requirement of our approach is the use of a heavy-ion accelerator (e.g., cyclotron or LINAC) that can deliver high-intensity heavy-ion beams in the energy range 10–20 MeV/nucleon. Fortunately, such accelerators are available at a number of facilities worldwide and, with appropriate planning, a fraction of their beam time may be devoted to non-standard radionuclide production following our inverse-kinematics approach.

We note that the use of the cryogenic gas cell has the additional advantage that its cooled windows can withstand the necessary high beam currents. Adequate circulation of the cooled hydrogen gas will be necessary to mitigate the effect of the local density reduction. For safe operation of the gas cell under intense beam irradiation, even with thinner windows, we may consider lowering the pressure to 1.0–1.5 atm, increasing the length, and, furthermore, lowering the temperature below LN_2 temperatures with the use of modern cryocoolers [e.g., a Gifford-McMahon refrigerator (Radebaugh (2009))].

Taking advantage of the development of thin liquids, it is conceivable to substitute the hydrogen gas cell with a liquid H_2 cell that has thin windows. The development of a liquid H_2/D_2 target with typical thickness of a few mm is reported in (Jaeckle et al. (1994)). More recently, a liquid H_2 target for fragmentation reactions has been reported in (Ryuto et al. (2005)). This target was operated at temperatures of about 20 K, achieved with a Gifford-McMahon refrigerator. The cell had a length of 30 mm and a density of 200 mg/cm³. We propose the implementation of a similar system for the production of medical isotopes, but for this purpose, the length has to be 1–2 mm to achieve the required thickness of about 8–10 mg/cm².

In regard to the Cyclotron Institute at TAMU, the facility houses two cyclotrons: a) the K150 cyclotron which can produce high-intensity heavy-ion beams (up to around Kr) with energies up to around 12–15 MeV/nucleon, suitable for the production of relatively large activities of radioisotopes and, b) the K500 cyclotron, employed in the present experiment, which can produce lower currents of heavy-ion beams (up to ^{238}U) and in a broader energy range (up to 20–40 MeV/nucleon depending on the isotope). We anticipate that both the K150 and the K500 cyclotrons may be successfully used for the development and production of a variety of non-standard radioisotopes at activities appropriate for medical studies on small animals. For this purpose, however, beams of 30–100 pnA have to be developed, which should be possible with a modest investment at the existing ion-source and accelerator

infrastructures.

To summarize, the aforementioned considerations for the development of a viable route of medical radioisotope production in inverse kinematics are based, first, on the successful results of the present study and second, on the current expertise and developments on ion-source and accelerator technologies worldwide. A promising application of our proposed method is achievable with timely planning and allocation of relatively modest resources. Along with the other production approaches, the proposed route may contribute to a broad and diversified program of production and use of non-standard medical radionuclides.

5. Conclusions

In this article, an innovative method for the production of important medical radioisotopes was presented. The approach is based on realizing the nuclear reaction in inverse kinematics by directing a heavy-ion beam of appropriate energy on a light target (e.g., H, d, He) and collecting the isotope of interest on an appropriate catcher after the target. In this work, as a proof-of-principle, we studied the production of the radionuclide ^{67}Cu ($T_{1/2} = 62$ h) via the reaction of a beam of 15 MeV/nucleon ^{70}Zn with a cryogenic hydrogen gas target. The ^{67}Cu radionuclide (along with other coproduced isotopes) was collected after the gas target on an Al catcher foil and the radioactivity was measured by off-line γ -ray analysis. After the end of the irradiation, the main radioimpurity in the Al catcher coming from the $^{70}\text{Zn} + \text{p}$ reaction was ^{69m}Zn ($T_{1/2} = 13.8$ h), which can be suppressed by cooling for a period of 2–3 days. Other identified radioimpurities came from the interaction of the beam with the window material and the catcher; these can be eliminated by careful tuning of the setup parameters. The present successful test and the ensuing considerations indicate the possibility of producing important non-standard radionuclides of high radionuclide purity with the approach of inverse kinematics. In parallel with the main production scheme, secondary neutrons from the primary reaction were used to irradiate a secondary target of Zn for further radioisotope production with promising results. The main requirement necessary to achieve production of activities appropriate for preclinical studies is the availability of high-intensity (particle μA) heavy-ion primary beams.

Acknowledgements

We are grateful to the support staff of the Cyclotron Institute for providing the primary beam. We thank Dr. H.T. Chifotides for inspiring discussions and suggestions, and for critical reading and editing of the manuscript. Financial support for this work was provided, in part by NNSA under grant no de-na0003841 (CENTAUR), and by the National and Kapodistrian University of Athens under the ELKE Research Account No 70/4/11395. M.Y. and P.Z.F. acknowledge the support of the Houston Methodist Research Institute (HMRI).

References

Agostinelli, S., et al., 2003. Geant4 a simulation toolkit. *Nucl. Instrum. Methods Phys. Res.* 506, 250–303.

Amadio, G., Yamaguchi, H., Wakabayashi, Y., Hayakawa, S., Kubono, S., 2008. Development of a cryogenic gas target for intense RI beam production at CRIB. *Nucl. Instrum. Methods Phys. Res.* 590, 191–193.

Asabella, A.N., Cascini, G.L., Altini, C., Paparella, D., Notaristefano, A., Rubini, G., 2014. The copper radioisotopes: a systematic review with special interest to ^{64}Cu . *BioMed Res. Int.* 2014, 786463.

Auditore, L., Amato, E., Baldari, S., 2017. Theoretical estimation of ^{64}Cu production with neutrons emitted during ^{18}F production with a 30MeV medical cyclotron. *Appl. Radiat. Isot.* 122, 229–234.

Brinkley, J.F., et al., 2009. Progress in Research. Cyclotron Institute, Texas A&M University (2002–2003), p. V-9 accessible at: <http://cyclotron.tamu.edu/publications.html>.

Carzaniga, T.S., Auger, M., Braccini, S., Bunka, M., Ereditato, A., Nesteruk, K.P., Scampoli, P., Turler, A., van der Meulen, N., 2017. Measurement of ^{43}Sc and ^{44}Sc production cross section with an 18 MeV medical PET cyclotron. *Appl. Radiat. Isot.* 129, 96–102.

Champion, C., Quinto, A.M., Morgat, C., Zanotti-Fregonara, P., Hindie, E., 2016. Comparison between three promising β -emitting radionuclides, ^{67}Cu , ^{47}Sc and ^{161}Tb , with emphasis on doses delivered to minimal residual disease. *Theranostics* 6 (4), 1611–1618.

Duchemin, C., Guertin, A., Haddad, F., Michel, N., Metivier, V., 2015. Production of medical isotopes from a thorium target irradiated by light charged particles up to 70 MeV. *Phys. Med. Biol.* 60, 931–946.

Follacchio, G.A., De Feo, M.S., De Vincentis, G., Monteleone, F., Liberatore, M., 2018. Radiopharmaceuticals labelled with copper radionuclides: clinical results in human beings. *Curr. Radiopharm.* 11 (1), 22–33.

Fountas, P.N., Souliotis, G.A., Veselsky, M., Bonasera, A., 2014. Systematic study of neutron-rich rare isotope production in peripheral heavy-ion collisions below the Fermi energy. *Phys. Rev. C* 90, 064613.

Gopalakrishna, A., Suryanarayana, S.V., Naik, H., Dixit, T.S., Nayak, B.K., Kumar, A., Maletta, P., Thakur, K., Deshpande, A., Ramamoorthy Krishnan, R., Kamaldeep, Banerjee, S., Saxena, A., 2018. Production, separation and supply prospects of ^{67}Cu with the development of fast neutron sources and photonuclear technology. *Radiochim. Acta* 106 (7), 549–557.

Hilgers, K., Stoll, T., Skakun, Y., Coenen, H.H., Qaim, S.M., 2003. Cross section measurements of the nuclear reactions $^{nat}\text{Zn}(\text{d},\text{p})^{64}\text{Cu}$, $^{66}\text{Zn}(\text{d},\alpha)^{64}\text{Cu}$, $^{68}\text{Zn}(\text{p},\text{cm})^{64}\text{Cu}$ for production of ^{64}Cu and technical developments for small scale production of ^{67}Cu via the $^{70}\text{Zn}(\text{p},\alpha)^{67}\text{Cu}$ process. *Appl. Radiat. Isot.* 59, 343–351.

Hosseini, S.F., Aboudzadeh, M., Sadeghi, M., Ahmadzadeh, M., Teymourlouy, A., Rostampour, M., 2017. Assessment and estimation of ^{67}Cu production yield via deuteron induced reactions on ^{nat}Zn and ^{70}Zn . *Appl. Radiat. Isot.* 127, 137–141.

Iacob, V.E., Hardy, J.C., Brinkley, J.F., Gagliardi, C.A., Mayes, V.E., Nica, N., Sanchez-Vega, M., Tabacaru, G., Trache, L., Tribble, R.E., 2006. Precise half-life measurements for the superallowed β^+ emitters ^{34}Ar and ^{34}Cl . *Phys. Rev. C* 74, 055502.

Iacob, V.E., Hardy, J.C., Banu, A., Chen, L., Golovko, V.V., Goodwin, J., Horvat, V., Nica, N., Park, H.I., Trache, L., Tribble, R.E., 2010. Precise half-life measurement of the superallowed β^+ emitter ^{26}Si . *Phys. Rev. C* 82, 035502.

Jaeckle, V., Kilian, K., Machner, H., Nake, Ch., Oelert, W., Turek, P., 1994. A liquid hydrogen/deuterium target with very thin windows. *Nucl. Instrum. Methods Phys. Res.* 349, 15–17.

Jamriska Sr., D.J., Taylor, W.A., Ott, M.A., Heaton, R., Phillips, D., Fowler, M., 1995. Activation rates and chemical recovery of ^{67}Cu produced with low energy proton irradiation of enriched ^{67}Zn targets. *J. Radioanal. Nucl. Chem.* 195, 263–270.

Jin, Z.H., Furukawa, T., Ohya, T., Degardin, M., Sugyo, A., Tsuji, A.B., Fujibayashi, Y., Zhang, M.R., Higashi, T., Boturyn, D., Dumy, P., Saga, T., 2017. ^{67}Cu -Radiolabeling of a multimeric RGD peptide for $\alpha V\beta 3$ integrin-targeted radionuclide therapy: stability, therapeutic efficacy, and safety studies in mice. *Nucl. Med. Commun.* 38 (4), 347–355.

Johnsen, A.M., Heidrich, B.J., Durrant, C.B., Bascom, A.J., Unlu, K., 2015. Reactor production of ^{64}Cu and ^{67}Cu using enriched zinc target material. *J. Radioanal. Nucl. Chem.* 305, 61.

Kastleiner, S., Koenen, H.H., Qaim, S.M., 1999. Possibility of production of ^{67}Cu at a small-sized cyclotron via the (p, α) reaction on enriched ^{70}Zn . *Radiochim. Acta* 84, 107–110.

Katabuchi, T., Watanabe, S., Ishioka, N.S., Iida, Y., Hanaoka, H., Endo, K., et al., 2008. Production of ^{67}Cu via the $^{68}\text{Zn}(\text{p},2\text{p})^{67}\text{Cu}$ reaction and recovery of ^{68}Zn target. *J. Radioanal. Nucl. Chem.* 277, 467–470.

Katz, B.M., Barnea, A., 1990. The ligand specificity for uptake of complexed copper-67 by brain hypothalamic tissue is a function of copper concentration and copper:ligand molar ratio. *J. Biol. Chem.* 265, 2017–2021.

Kawabata, M., Hashimoto, K., Saeki, H., Sato, N., Motoishi, S., Nagai, Y., 2015. Production and separation of ^{64}Cu and ^{67}Cu using 14 MeV neutrons. *J. Radioanal. Nucl. Chem.* 303, 1205.

Kawrakow, I., 2000. Accurate condensed history Monte Carlo simulation of electron transport. I. EGSnrc, the new EGS4 version. *Med. Phys.* 27, 485.

Kawrakow, I., Rogers, D.W.O., 2003. NRCC Report PIRS-701, NRC, Ottawa. accessible at: <https://nrc-cncr.github.io/EGSnrc/>.

Kin, T., Nagai, Y., Iwamoto, N., Minato, F., Iwamoto, O., Hatsuoka, Y., Segawa, M., Harada, H., Konno, C., Ochiai, K., Takakura, K., 2013. New production routes for medical isotopes ^{64}Cu and ^{67}Cu using accelerator neutrons. *J. Phys. Soc. Jpn.* 82, 034201.

Knogler, K., Grunberg, J., Zimmermann, K., Cohrs, S., Honer, M., Ametamey, S., Altevogt, P., Fogel, M., Schubiger, P.A., Novak-Hofer, I., 2007. Copper-67 radioimmunotherapy and growth inhibition by anti L1-cell adhesion molecule monoclonal antibodies in a therapy model of ovarian cancer metastasis. *Clin. Cancer Res.* 13 (2), 603–611.

Koning, A.J., Rochman, D., 2012. Modern nuclear data evaluation with the TALYS code system. *Nucl. Data Sheets* 113 (12), 28412934.

Kozempel, J., Abbas, K., Simonelli, F., Bulgheroni, A., Holzwarth, U., Gibson, N., 2012. Preparation of ^{67}Cu via deuteron irradiation of ^{70}Zn . *Radiochim. Acta* 100, 419–423.

Leon, A., et al., 1998. Charge state distributions of swift heavy ions behind various solid targets. *Atomic Data Nucl. Data Tables* 69, 217–238.

Linder, M.C., 1991. Biochemistry of Copper, first ed. Plenum Press, NY.

Mastren, T., Pen, A., Peaslee, G.F., Wozniak, N., Loveless, S., Essemacher, S., Sobotka, L.G., Morrissey, D.J., Lapi, S.E., 2014. Feasibility of isotope harvesting at a projectile fragmentation facility: ^{67}Cu . *Sci. Rep.* 4 (6706), 1–6.

Mastren, T., Pen, A., Loveless, S., Marquez, B.V., Bollinger, E., Marois, B., Hubley, N., Brown, K., Morrissey, D.J., Peaslee, G.F., Lapi, S.E., 2015. Harvesting ^{67}Cu from the collection of a secondary beam cocktail at the national superconducting cyclotron laboratory. *Anal. Chem.* 87 (20), 10323–10329.

Medvedev, D.G., Mausner, L.F., Meinken, G.E., Kurczak, S.O., Schnakenberg, H., Dodge, C.J., et al., 2008. Development of a large scale production of ^{67}Cu from ^{68}Zn at the high energy proton accelerator: closing the ^{68}Zn cycle. *Appl. Radiat. Isot.* 70, 423–429.

Mirzadeh, S., Mausner, L.F., Srivastava, S.C., 1986. Production of no-carrier added ^{67}Cu . *Appl. Radiat. Isot.* 37 (1986), 29.

Novak-Hofer, I., Schubiger, P.A., 2002. Copper-67 as a therapeutic nuclide for radioimmunotherapy. *Eur. J. Nucl. Med. Mol. Imaging* 29 (6), 821–830.

O'Brien, H.A., 1969. The preparation of ^{67}Cu from ^{67}Zn in a nuclear reactor. *Int. J. Appl. Radiat. Isot.* 20, 121–124.

Ohya, T., Nagatsu, K., Suzuki, H., Fukada, M., Minegishi, K., Hanyu, M., Zhang, M.R., 2018. Small-scale production of ^{67}Cu for a preclinical study via the $^{64}\text{Ni}(\alpha, p)^{67}\text{Cu}$ channel. *Nucl. Med. Biol.* 59, 56–60.

Papageorgiou, A., Souliotis, G.A., Tshoo, K., Jeong, S.C., Kang, B.H., Kwon, Y.K., Veselsky, M., Yennello, S.J., Bonasera, A., 2018. Neutron-rich rare isotope production with stable and radioactive beams in the mass range $A = 40$ – 60 at beam energy around 15 MeV/nucleon. *J. Phys. G Nucl. Part. Phys.* 45, 095105 25pp.

Peng, F., Lu, X., Janisse, J., Muzik, O., Shields, A.F., 2006. PET of human prostate cancer xenografts in mice with increased uptake of $^{64}\text{CuCl}_2$. *J. Nucl. Med.* 47, 1649.

Price, E.W., Orvig, C., 2014. Matching chelators to radiometals for radiopharmaceuticals. *Chem. Soc. Rev.* 43, 260.

Pupillo, G., Sounalet, T., Michel, N., Mou, L., Esposito, J., Haddad, F., 2018. New production cross sections for the theranostic radionuclide ^{67}Cu . *Nucl. Instrum. Methods Phys. Res. B* 415, 41–47.

Qaim, S.M., 2017. Nuclear data for production and medical application of radionuclides: present status and future needs. *Nucl. Med. Biol.* 44, 31–49.

Radebaugh, R., 2009. Cryocoolers: the state of the art and recent developments. *J. Phys. Condens. Matter* 21, 164219 9pp.

Rodrigues, M.R.D., Souliotis, G.A., Wang, K., Iakob, V., Nica, N., Roedder, B., Tabacaru, G., Yu, M., Zanotti-Fregonara, P., Bonasera, A., 2019. A Novel Dual Approach to Medical Radioisotope Production Employing Inverse Kinematics and the Secondary Emitted Neutrons. A Successful Test to Produce the Medical Radionuclide ^{67}Cu . (in preparation).

Ryuto, H., Kunibu, M., Minemura, T., Motobayashi, T., Sagara, K., Shimura, S., Tamaki, M., Yanagisawa, Y., Yano, Y., 2005. Liquid hydrogen and helium targets for radioisotope beams at RIKEN Nucl. Instrum. Methods Phys. Res. A 555, 1–5.

Sato, N., Tsukada, K., Watanabe, S., Ishioka, N.S., Kawabata, M., Saeki, H., Nagai, Y., Kin, T., Minato, F., Iwamoto, N., Iwamoto, O., 2014. First measurement of the radioisotope purity of the therapeutic isotope ^{67}Cu produced by $^{nat}\text{Zn}(n, x)$ reaction using $^{nat}\text{C}(d, n)$ neutrons. *J. Phys. Soc. Jpn.* 83, 073201.

Schubiger, P.A., Alberto, R., Smith, A., 1996. Vehicles, chelators and radionuclides: choosing the "building blocks" of an effective therapeutic radioimmunoconjugate. *Bioconjug. Chem.* 7, 165–179.

Skakun, Y., Qaim, S.M., 2004. Excitation function of the $^{64}\text{Ni}(\alpha, p)^{67}\text{Cu}$ reaction for production of ^{67}Cu . *Appl. Radiat. Isot.* 60, 33–39.

Smith, N.A., Bowers, D.L., Ehst, D.A., 2012. The production, separation, and use of ^{67}Cu for radioimmunotherapy: a review. *Appl. Radiat. Isot.* 70, 2377–2383.

Spahn, I., Coenen, H.H., Qaim, S.M., 2004. Enhanced production possibility of the therapeutic radionuclides ^{64}Cu , ^{67}Cu and ^{89}Sr via (n, p) reactions induced by fast spectral neutrons. *Radiochim. Acta* 92, 183.

Srivastava, S.C., 2014. Paving the way to personalized medicine: production of some theragnostic radionuclides at Brookhaven National Laboratory. *Radiochim. Acta* 99, 635.

Starovoitova, V.N., Tchelidze, L., Wells, D.P., 2014. Production of medical radioisotopes with linear accelerators. *Appl. Radiat. Isot.* 85, 39–44.

Starovoitova, V.N., Cole, P.L., Grimm, T.L., 2015. Accelerator-based photoproduction of promising beta-emitters ^{67}Cu and ^{47}Sc . *J. Radioanal. Nucl. Chem.* 305 (1), 127–132.

Stocklin, G., Qaim, S.M., Rosch, F., 1995. The impact of radioactivity on medicine. *Radiochim. Acta* 70/71, 249.

Stoll, T., Kastleiner, S., Shubin, Y.N., Coenen, H.H., Qaim, S.M., 2002. Excitation functions of proton induced reactions on ^{68}Zn from threshold up to 71 MeV, with specific reference to the production of ^{67}Cu . *Radiochim. Acta* 90, 309–313.

Sugo, Y., Hashimoto, K., Kawabata, M., Saeki, H., Sato, S., Tsukada, K., Nagai, Y., 2017. Application of ^{67}Cu produced by $^{68}\text{Zn}(n, np; d)^{67}\text{Cu}$ to biodistribution study in tumor-bearing mice. *J. Phys. Soc. Jpn.* 86, 023201.

Ting, G., Chang, C.H., Wang, H.E., 2009. Cancer nanotargeted radiopharmaceuticals for tumor imaging and therapy. *Anticancer Res.* 29, 4107–4118.

Trible, R.E., Burch, R.H., Gagliardi, C.A., 1989. MARS: a momentum achromat recoil spectrometer. *Nucl. Instrum. Methods A* 285, 441–446.

Uddin, Md S., Rumman-uz-Zaman, Md, Hossain, S.M., Qaim, S.M., 2014. Radiochemical measurement of neutron-spectrum averaged cross sections for the formation of ^{64}Cu and ^{67}Cu in the (n, p) reaction at a TRIGA Mark-II reactor: feasibility of simultaneous production of the theragnostic pair $^{64}\text{Cu}/^{67}\text{Cu}$. *Radiochim. Acta* 102, 473.

Yagi, M., Kondo, K., 1978. Preparation of carrier-free ^{67}Cu by the $^{68}\text{Zn}(\gamma, p)$ reaction. *Int. J. Appl. Radiat. Isot.* 29, 757.

Ziegler, J.F., Ziegler, M.D., Biersack, J.P., 2013. The stopping and range of ions in matter. Available at: <http://www.srim.org>.

Zimmermann, K., Grunberg, J., Honer, M., Ametamey, S., Schubiger, P.A., Novak-Hofer, I., 2003. Targeting of renal carcinoma with $^{67/64}\text{Cu}$ -labeled anti-L1-CAM antibody chCE7: selection of copper ligands and PET imaging. *Nucl. Med. Biol.* 30 (4), 417–427.